

QUANTIFYING THE LIKELIHOOD OF SUBSTRUCTURE IN CORONAL LOOPS

Kathryn McKeough¹

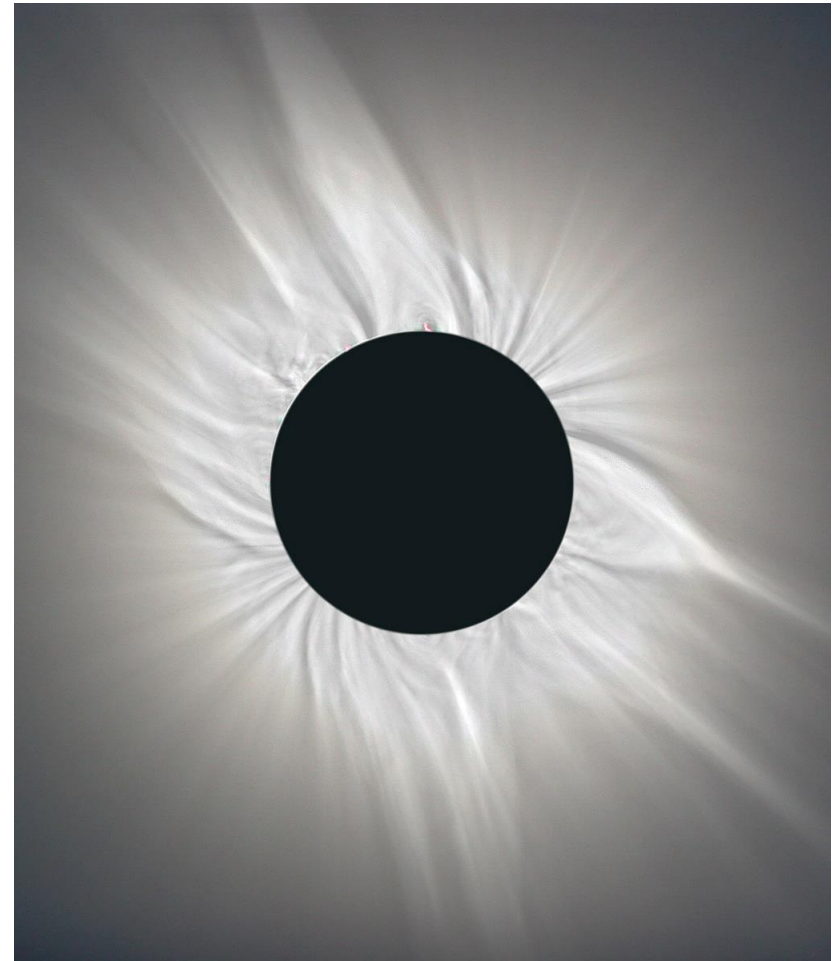
Vinay Kashyap² & Sean McKillop²

1 Carnegie Mellon University, 5000 Forbes Ave, Pittsburgh, PA 15289, USA

2 Harvard-Smithsonian Center for Astrophysics, 60 Garden St, Cambridge, MA 02138, USA

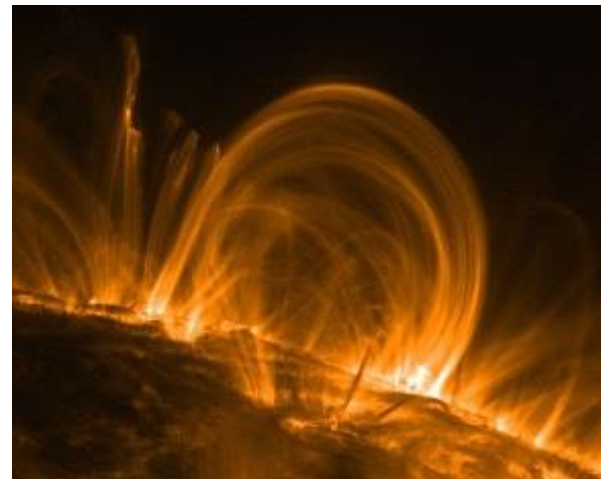
Coronal Heating

- 500,000 - 3 million K
- 1000 times hotter than surface of sun
- Power required =
 $\sim 1 \text{ kilowatt/m}^2$



Coronal Loops

- Magnetic flux tube filled with hot plasma
- Connects regions of opposite polarity
- Potential location of coronal heating mechanisms



Coronal Heating -Solutions

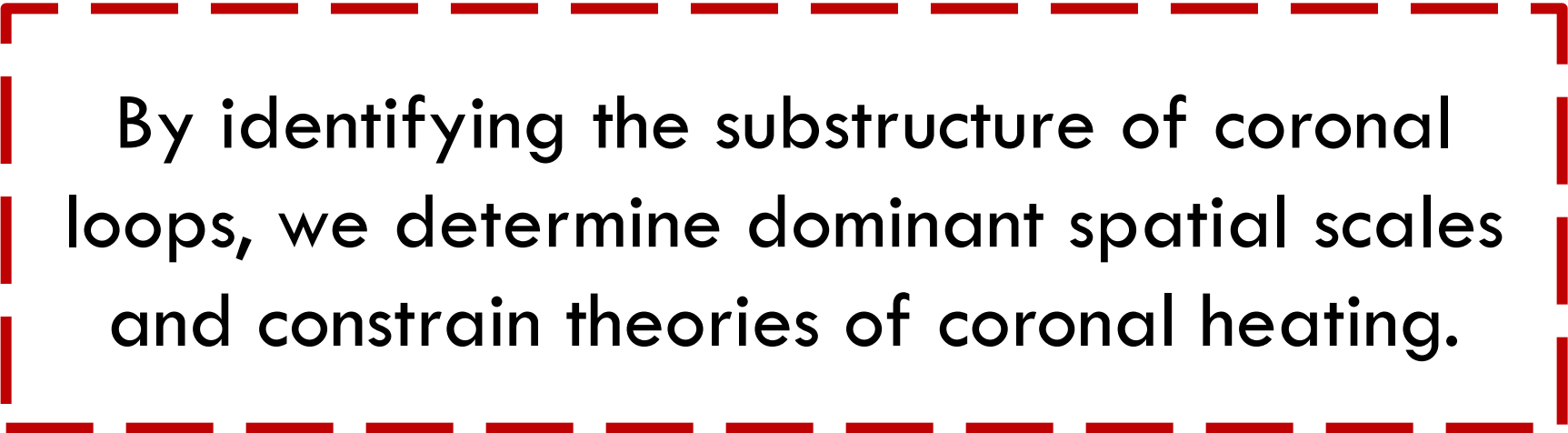
Nanoflares

- *Small scale*
- Small consecutive bursts of energy that contributes to heating
- Magnetic reconnection induced by stresses from footpoint motions causing braids in flux tubes

Alfven Waves

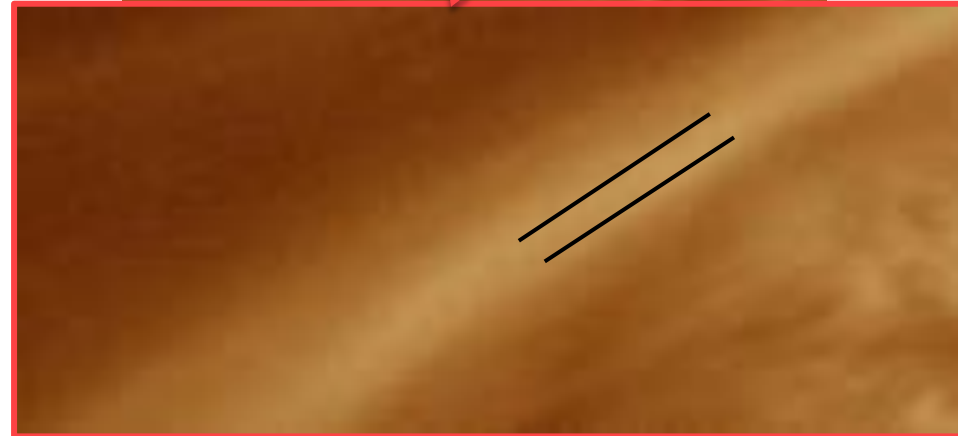
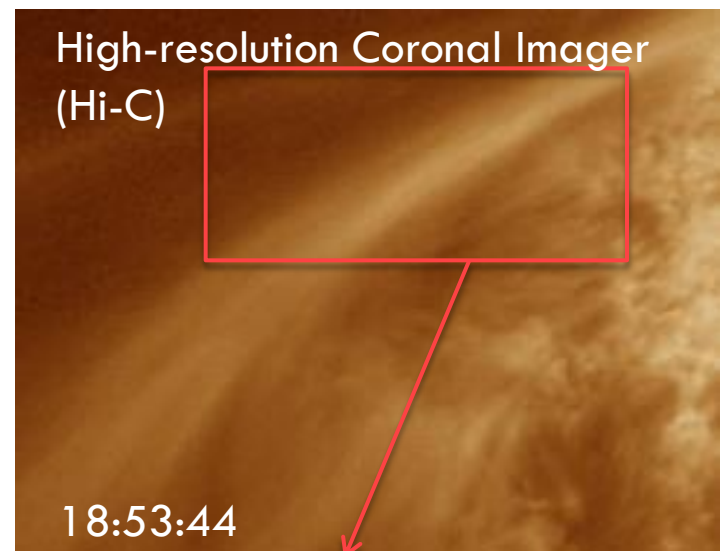
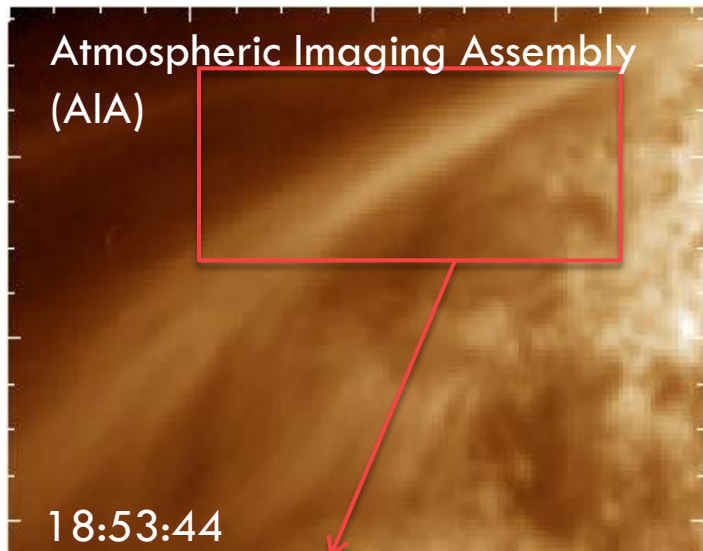
- *Large scale*
- Alfven waves dissipate energy into plasma through turbulence
- Waves propagate along flux tubes

Goal

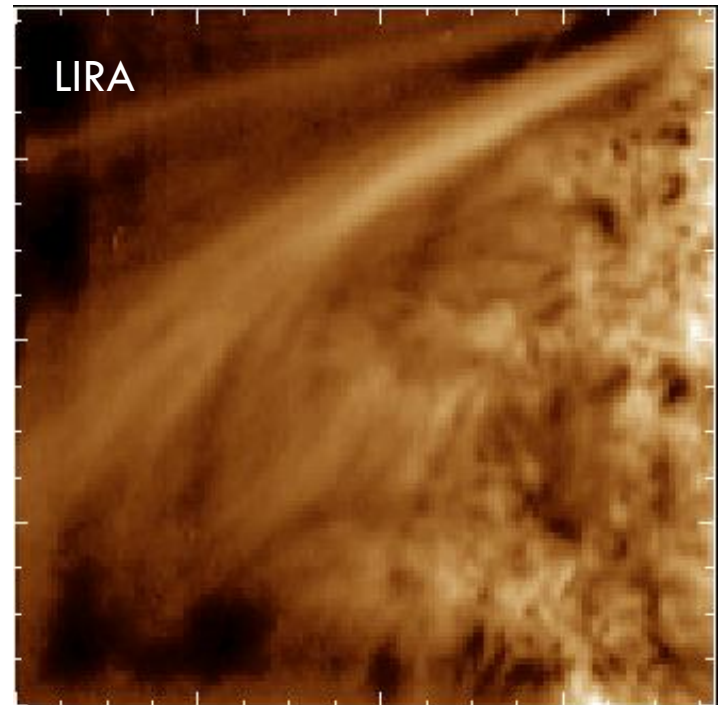
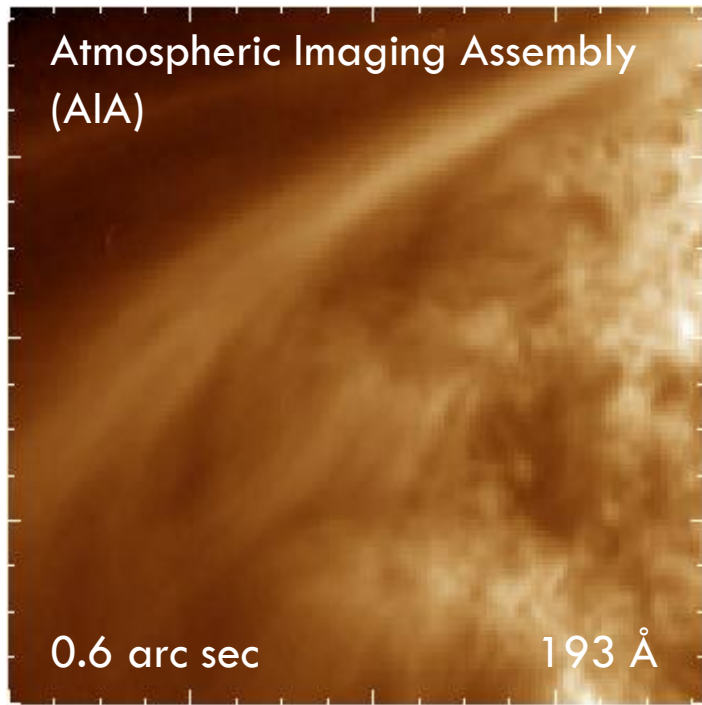


By identifying the substructure of coronal loops, we determine dominant spatial scales and constrain theories of coronal heating.

Increased Spatial Resolution



Increased Spatial Resolution



Low-Count Image Reconstruction and Analysis (LIRA)

- Bayes / Markov Chain Monte Carlo
- Two components
 - ▣ 1 smooth underlying baseline
 - ▣ Inferred multi-scale component

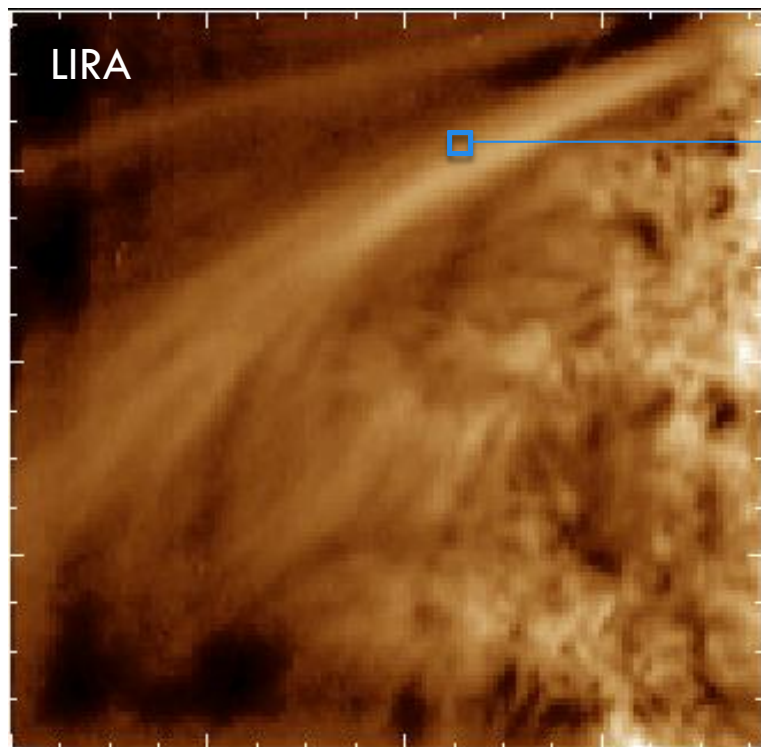
Esch et al. 2004

Connors & van Dyk 2007

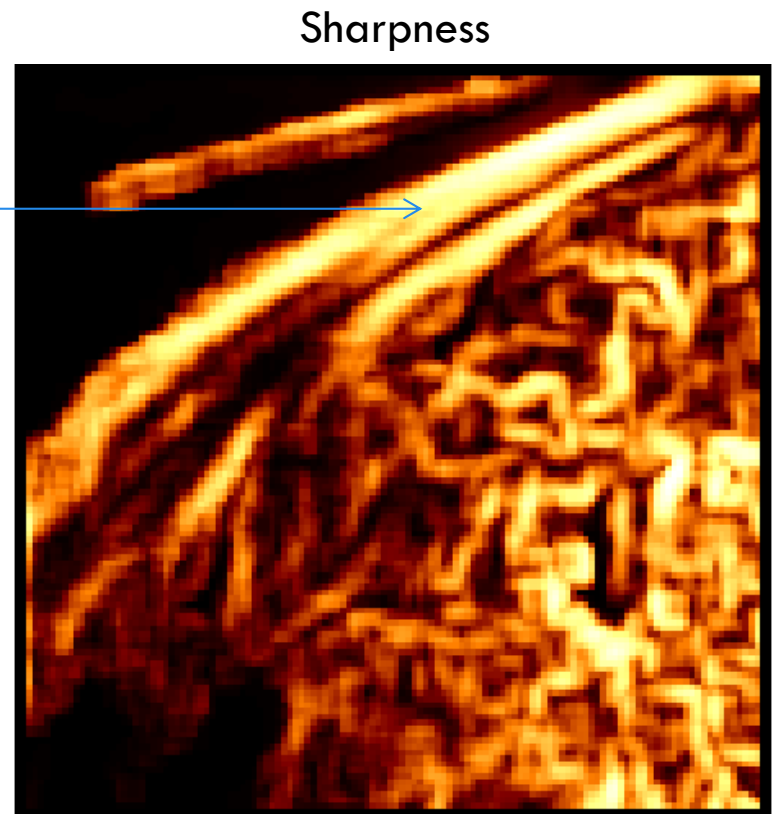
'Sharpness' Value

Wee & Paramesran 2008

- Quantify the prominence of the substructure



$$\psi_{i,j}$$



Gradient Correction

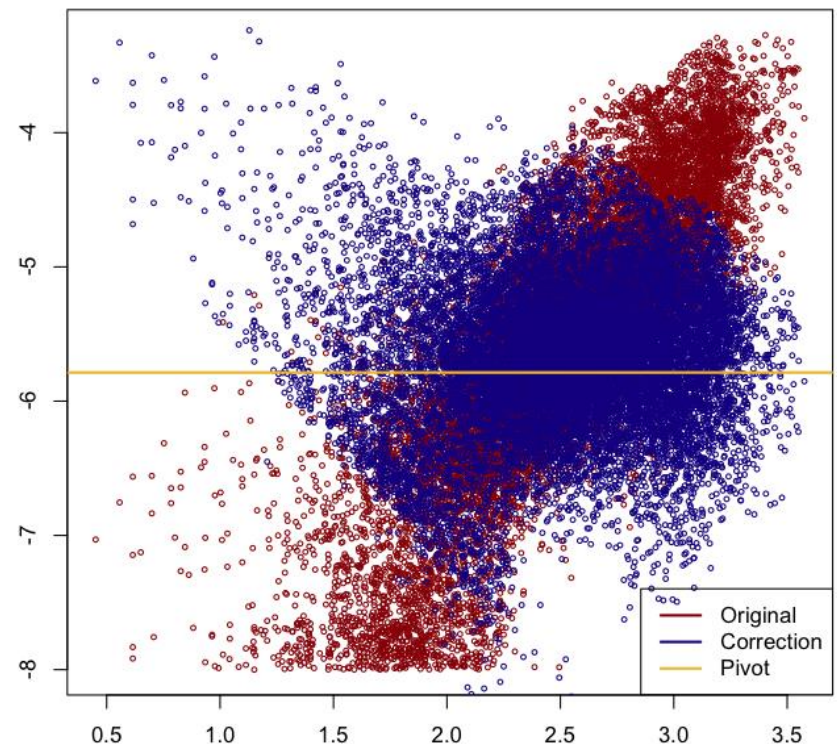
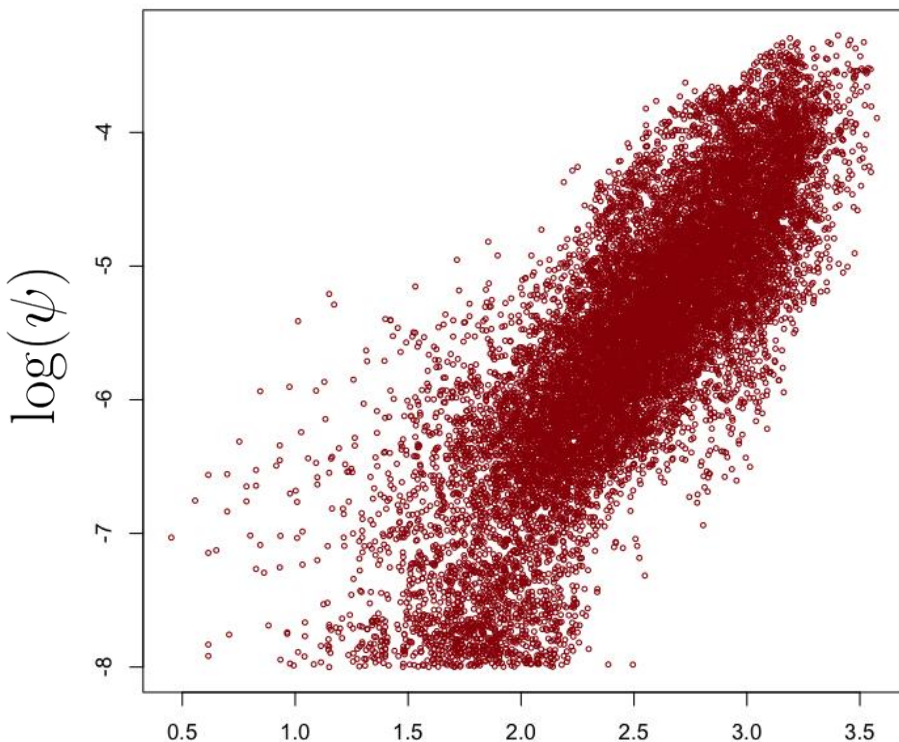
Linear Regression in
log-log space



Apply transformation
to sharpness

Sharpness v. Gradient

Sharpness v. Gradient

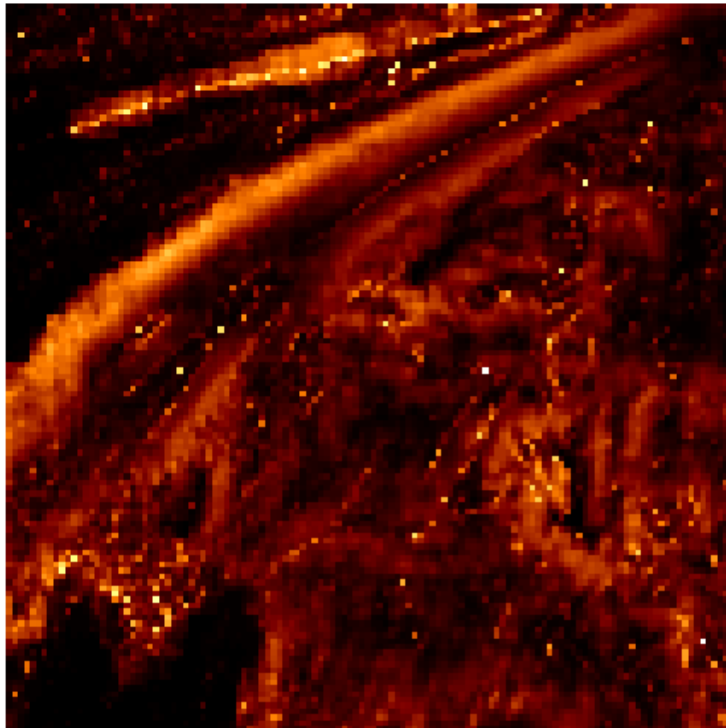


$\log(\nabla g(x, y))$

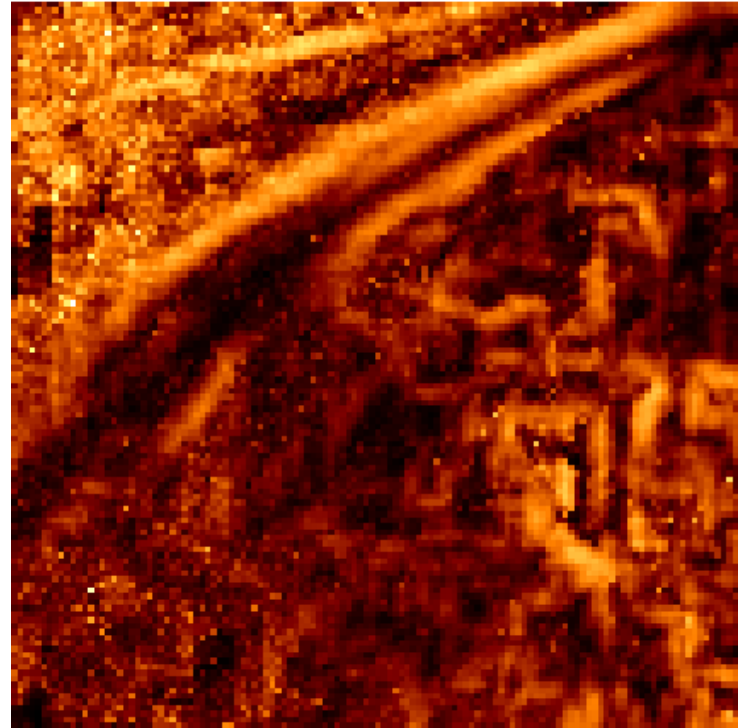
Significance of Substructure

- Null hypothesis = no substructure in coronal loop
- Null image = convolve observed image with PSF

LIRA on Observed
Corrected Sharpness



LIRA on Null Image
Corrected Sharpness

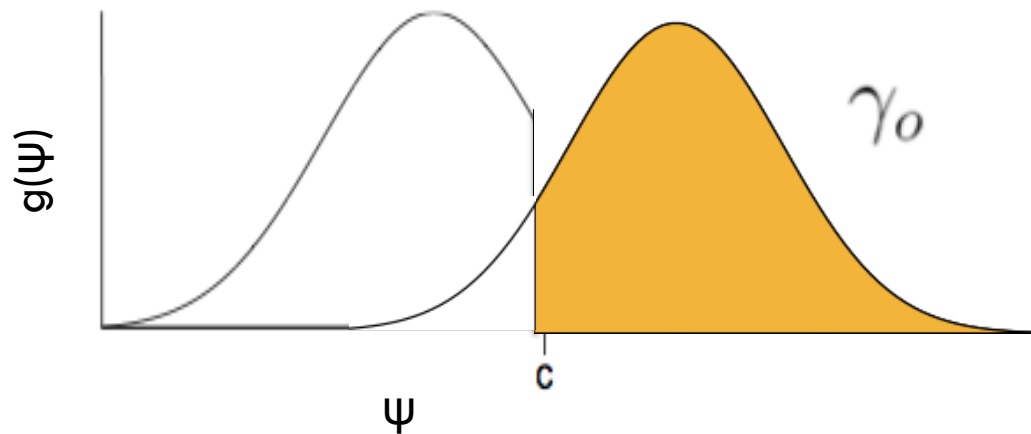


p-Value Upper Bound

Stein et al. 2014 (draft)

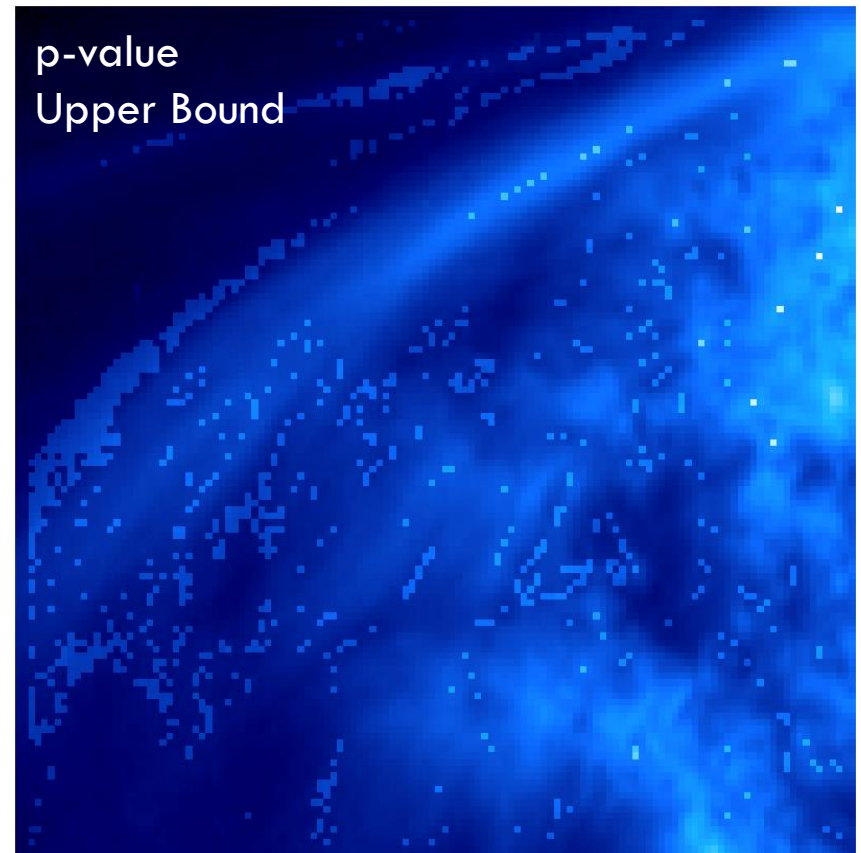
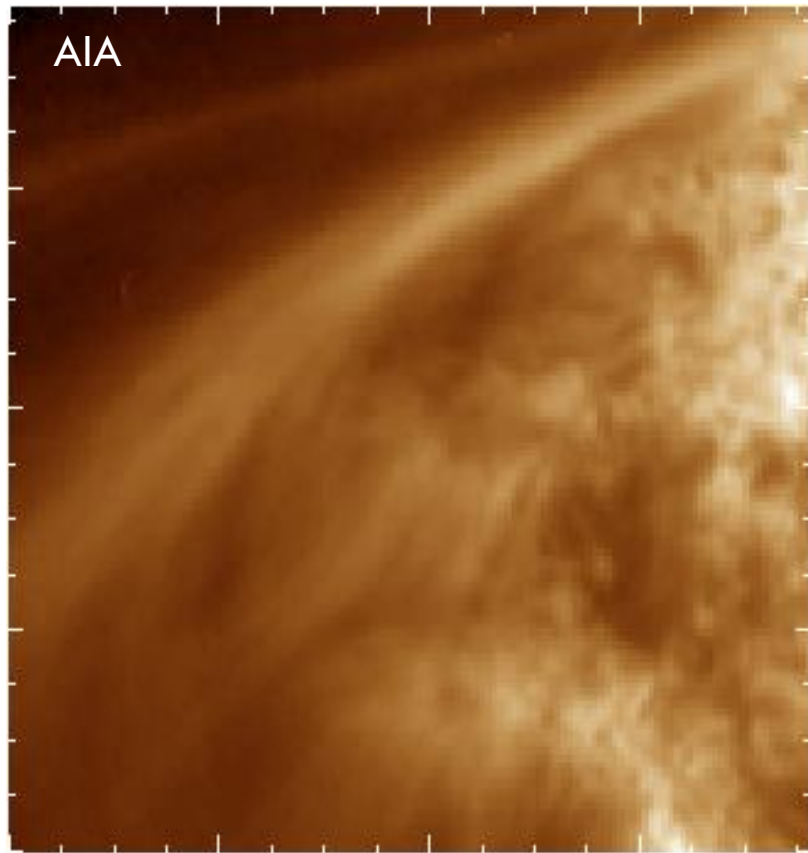
- 5 Poisson realizations of double convolved image
- Compare sharpness for the observed image (Ψ_o) and the simulated images (Ψ_n)

$$\boxed{\text{p-value upper bound}} \quad \hat{u} = \frac{\gamma_n}{\gamma_o}$$



p-Value Upper Bound

- Significant sharpness: $\hat{u} < 0.06$

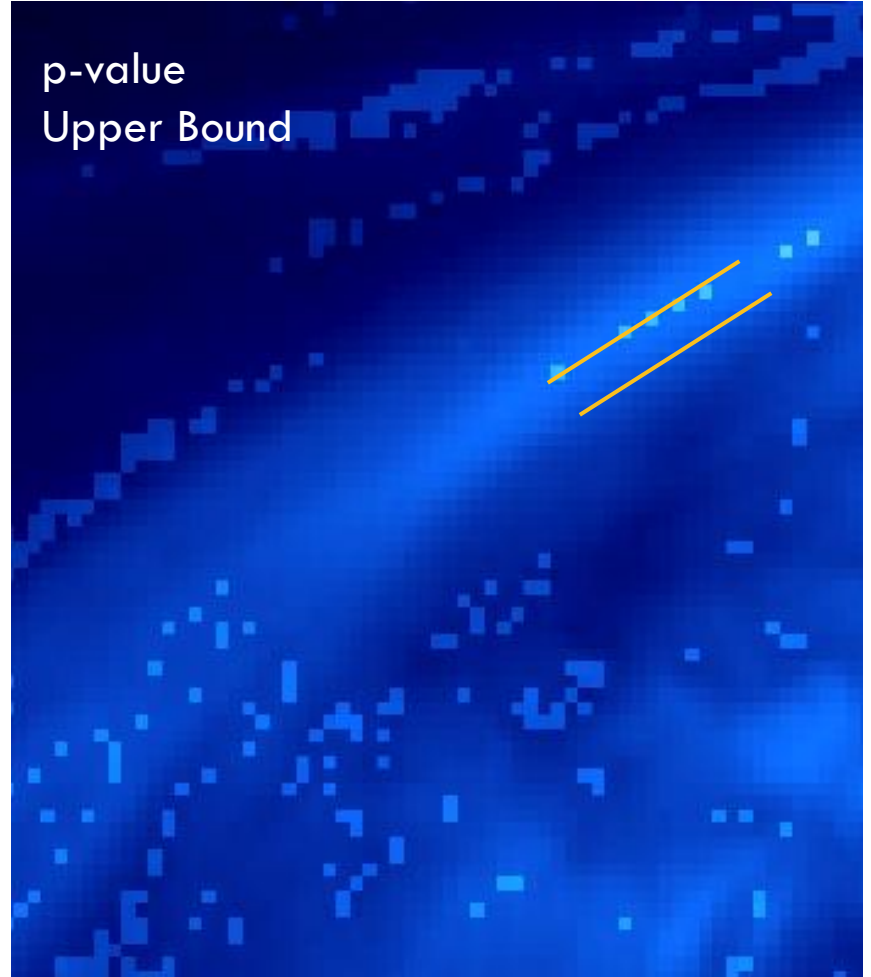


Hi-C Comparison

Hi-C

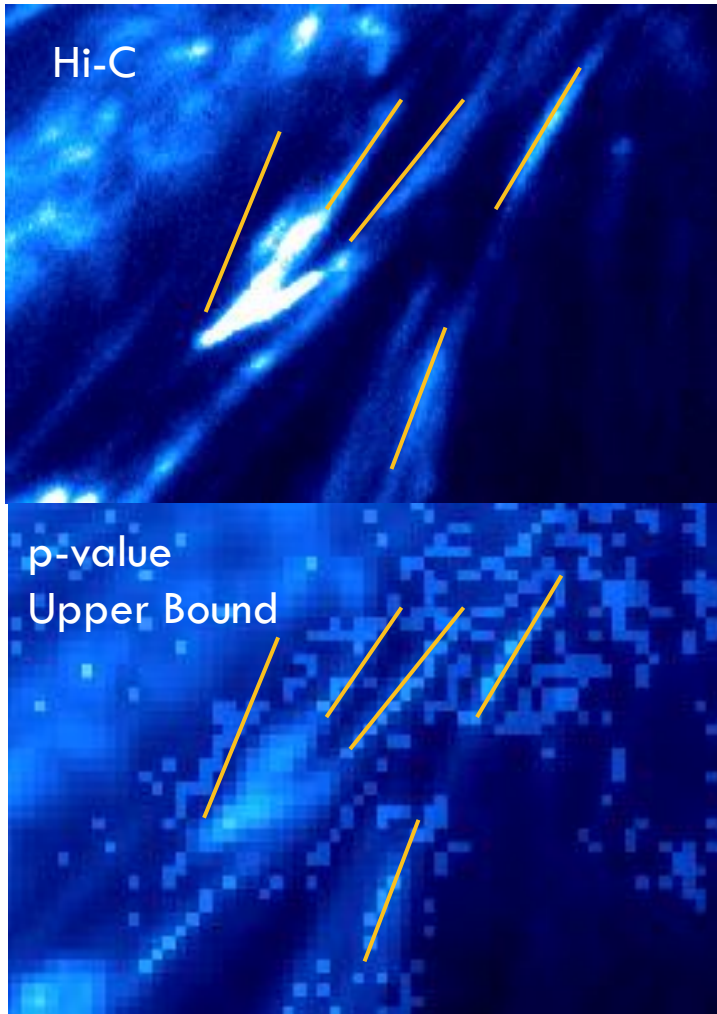


p-value
Upper Bound

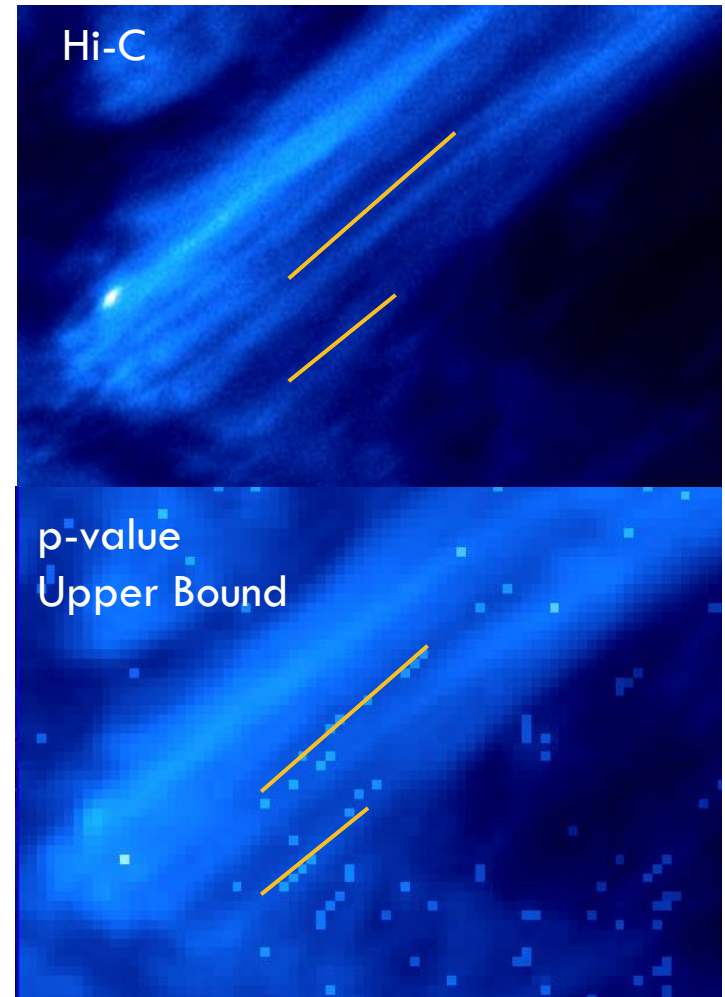


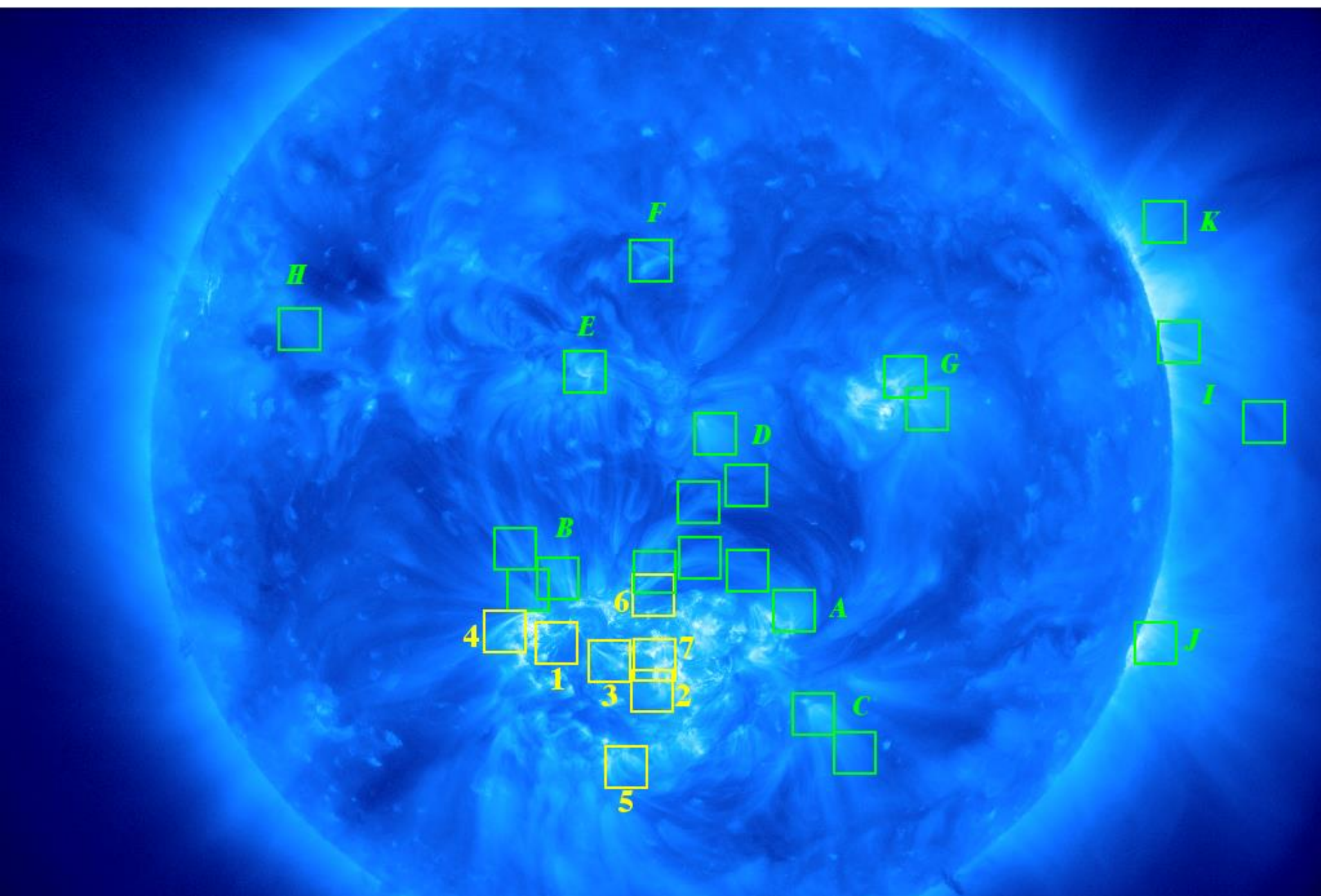
Hi-C Comparison

Trial 1

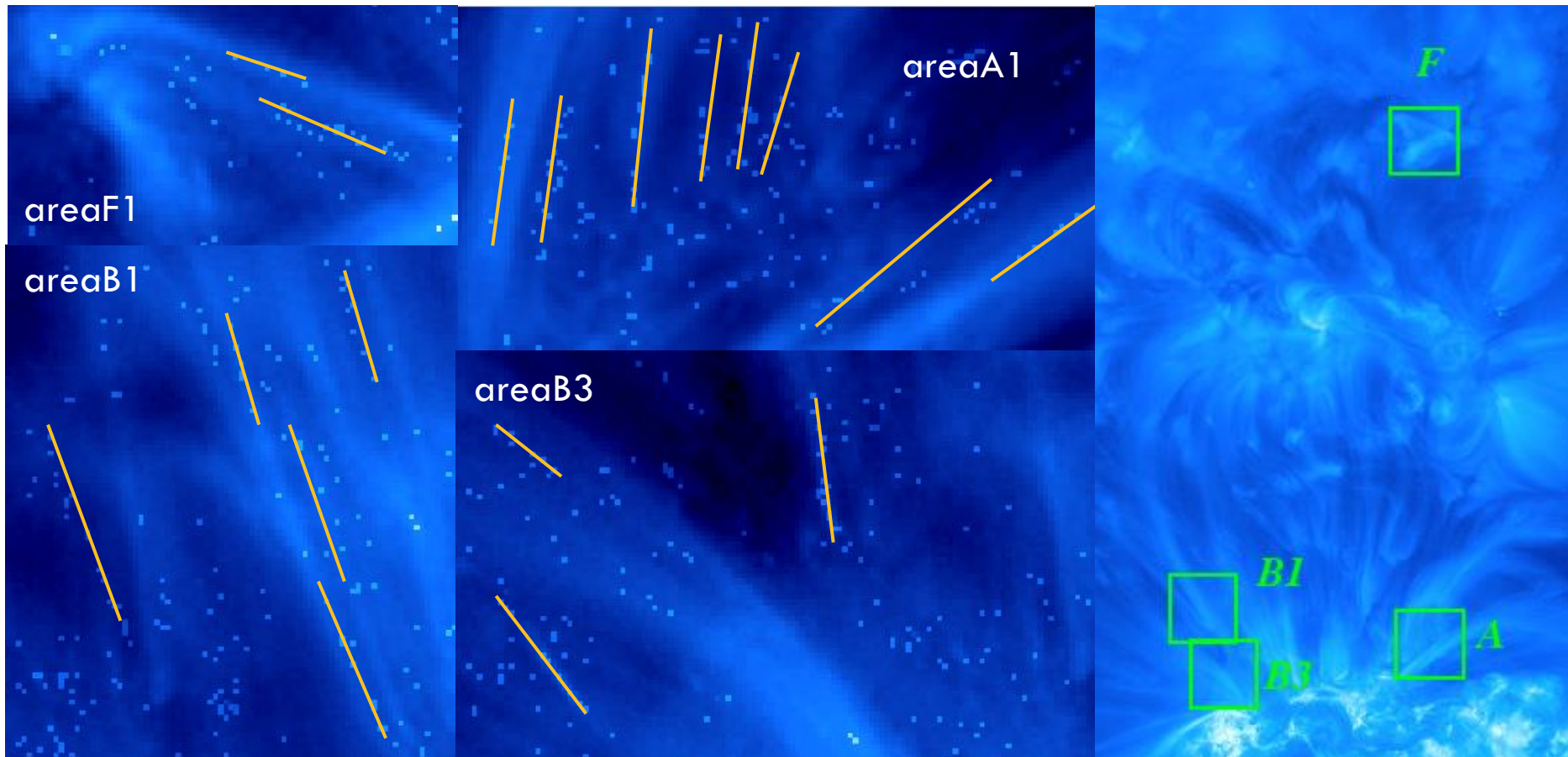


Trial 6





Detected Loops



Summary

- Developed method to search for substructure in solar images
- Found evidence for substructure in AIA images that we observe in Hi-C
- Similar evidence of substructure in AIA loops outside of Hi-C region:
 - ▣ Loops with strands appear to be ubiquitous
 - ▣ Supports nanoflare model
- Not all loops found to have substructure – unclear if statistical or physical explanation
- Isolated points possibly result of Poisson artifacts

Future Work

- Results are preliminary
 - ▣ Quantify false positives and non-detections
 - ▣ Increasing power could expand detection regions
- Understand implications of results
 - ▣ Relation between bright points and detections – compare significant pixel light curves
 - ▣ Why some loop complexes show no detections

Acknowledgements

We acknowledge support from AIA under contract SP02H1701R from Lockheed-Martin to SAO.

We acknowledge the High resolution Coronal Imager instrument team for making the flight data publicly available. MSFC/NASA led the mission and partners include the Smithsonian Astrophysical Observatory in Cambridge, Mass.; Lockheed Martin's Solar Astrophysical Laboratory in Palo Alto, Calif.; the University of Central Lancashire in Lancashire, England; and the Lebedev Physical Institute of the Russian Academy of Sciences in Moscow.

Vinay Kashyap acknowledges support from NASA Contract to Chandra X-ray Center NAS8-03060 and Smithsonian Competitive Grants Fund 40488100HH0043.

We thank David van Dyk and Nathan Stein for useful comments and help with understanding the output of LIRA.



Bibliography

Brooks, D. et al. 2013, ApJ, 722L, 19B

Cargill, P., & Klimchuck, J. 2004, ApJ, 605, 911C

Connors, A., & van Dyk, D. A. 2007, Statistical Challenges in Modern Astronomy IV, 371, 101

Cranmer, S., et al. 2012, ApJ, 754, 92C

Cranmer, S., et al. 2007, ApJS, 171, 520C

DeForest, C. E. 2007, ApJ, 661, 532D

Esch, D. N., Connors, A., Karovska, M., & van Dyk, D. A. 2004, ApJ, 610, 1213

Pastourakos, S., & Klimchuk, J. 2005, ApJ, 628, 1023P

Raymond, J. C., et al. 2014, ApJ, 788, 152R

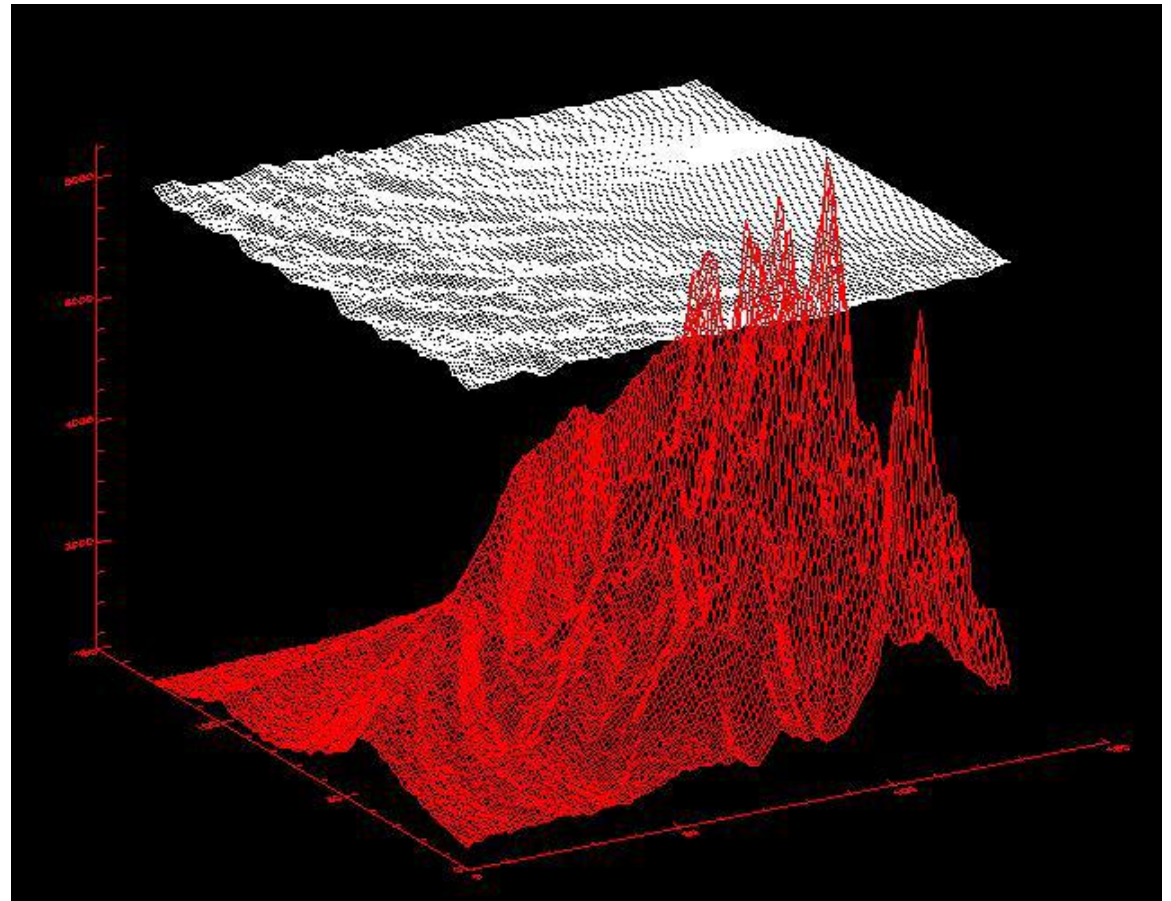
Viall, N. M., & Klimchuck J. 2011, ApJ, 738, 24V

Wee, C. Y., & Paramesran, R. 2008, ICSP2008 Proceedings, 978-1-4244-2179-4/08

Extra Slides

Baseline Model

1. Begin with max
2. Correct using min curvature surface through convex hull
3. Iterate until surface lies below data



LIRA Operations

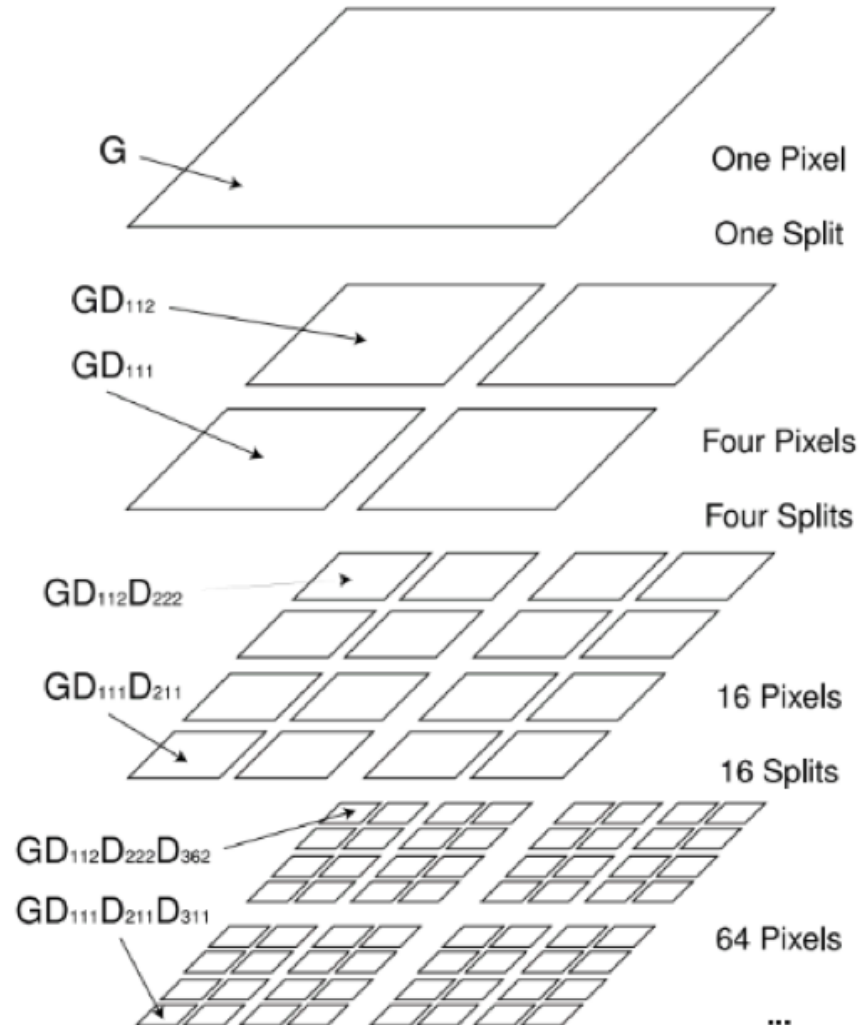
INPUT

- Point Spread Function (PSF)
- Observed Image ($2^n \times 2^n$)
- Baseline Model
- Prior & Starting Image

OUTPUT

- MCMC iterations of Multi-scale Counts
 - ▣ Posterior distribution of departures from baseline
 - ▣ De-convolution

Multi-scale Representation



'Sharpness' Value

$g(x, y)$ \longrightarrow Image matrix

$\tilde{g}(x, y) = \frac{g(x, y)}{\sqrt{\sum_{x=0}^{N-1} \sum_{y=0}^{N-1} [g(x, y)]^2}}$ \longrightarrow Normalization

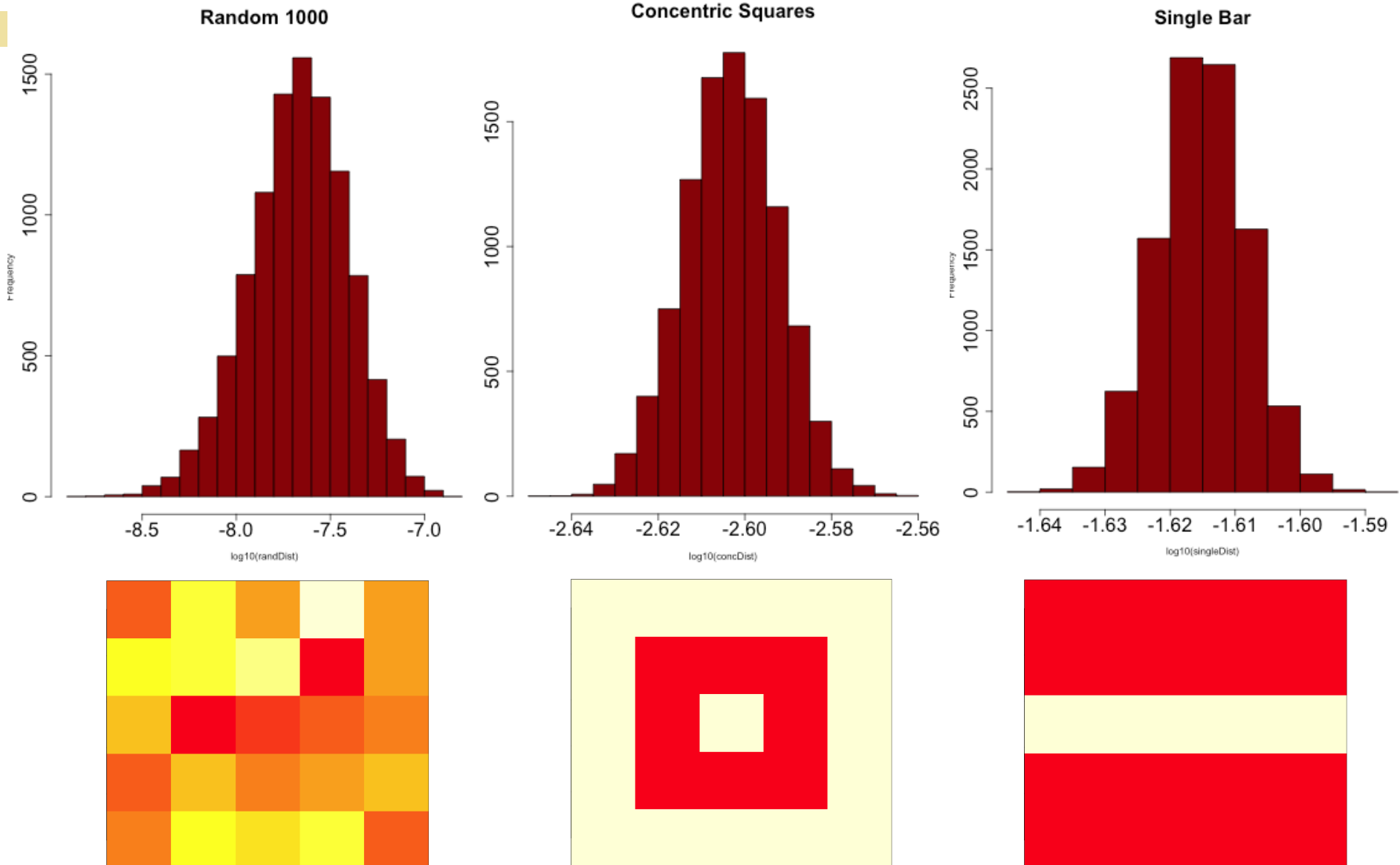
$G = \tilde{g}(x, y) - \mu$ \longrightarrow Subtract mean

$S_{\tilde{g}} = \frac{1}{(N-1)} GG^T$ \longrightarrow Covariance matrix

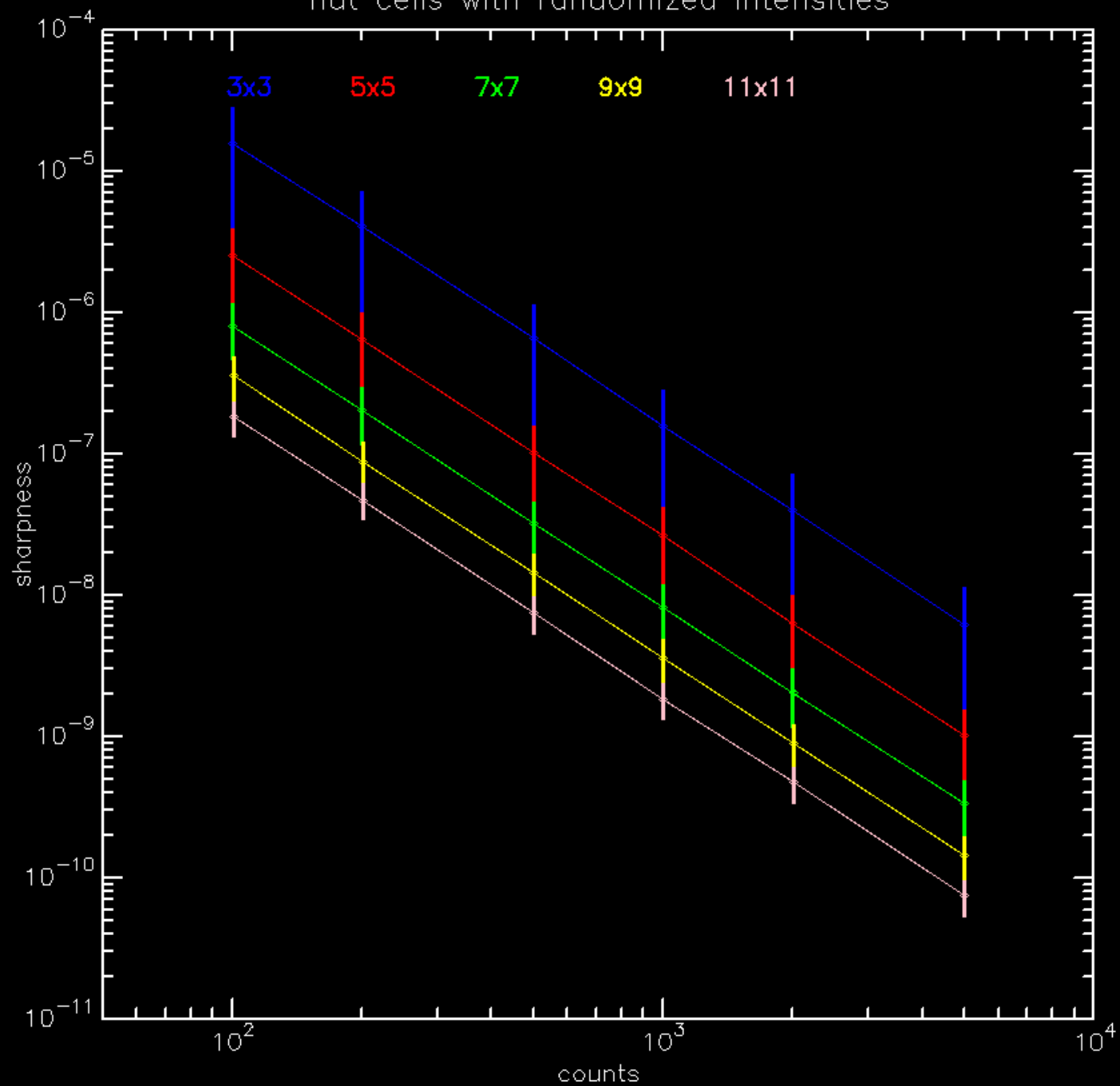
$S_{\tilde{g}} = UDV$ \longrightarrow Singular Value Decomposition

$\sum^N \lambda^2 = \psi$ \longrightarrow Sum of squared eigenvalues
(diagonal of D)

Sharpness & Structure Dependence

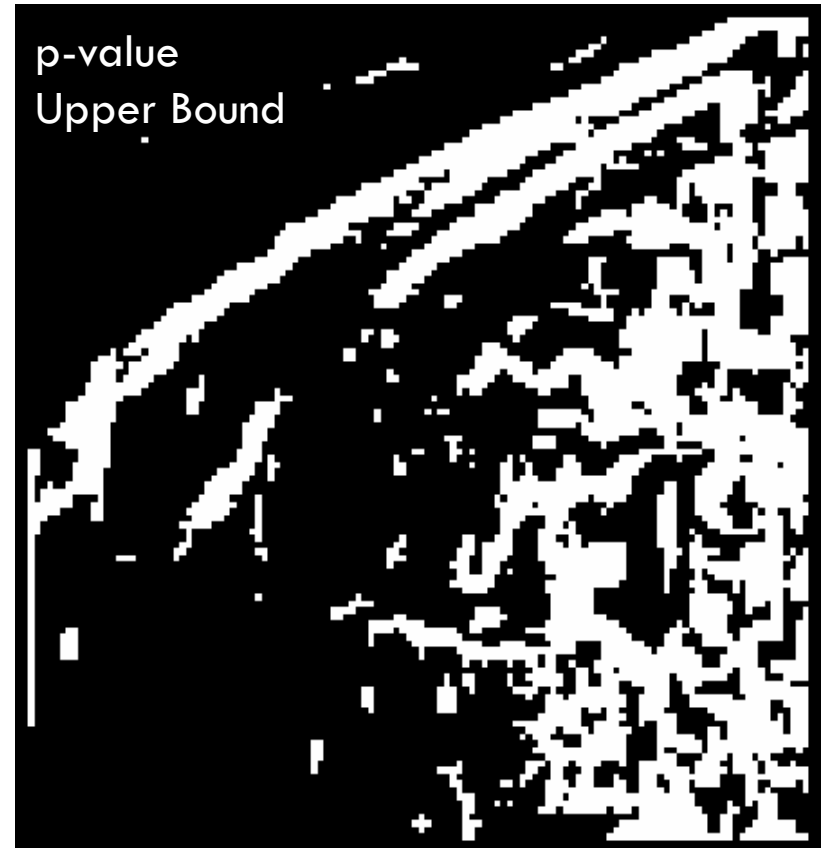
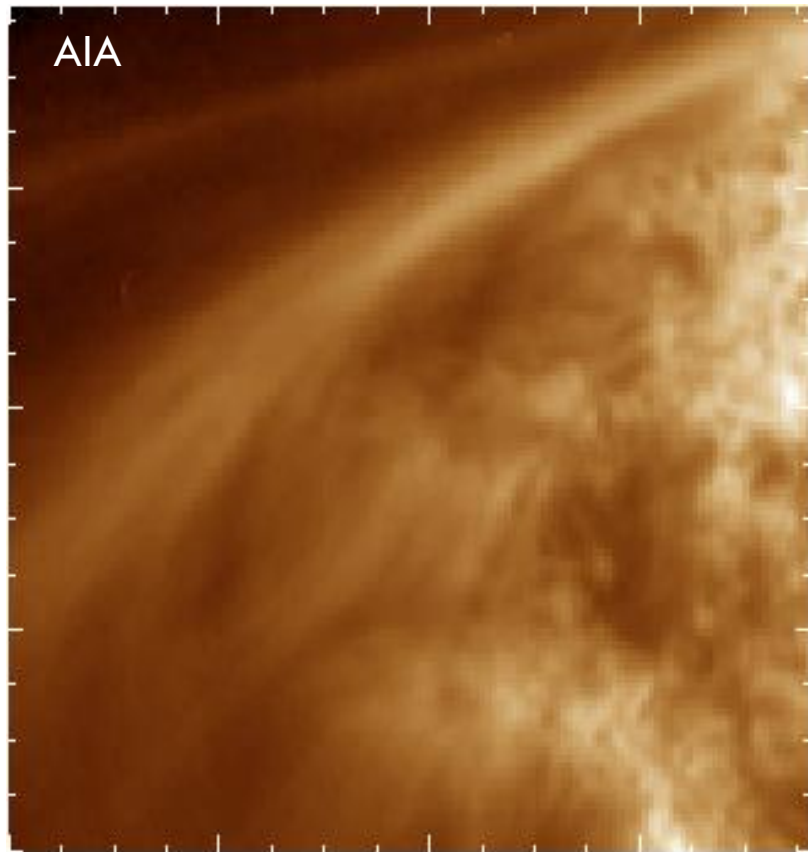


flat cells with randomized intensities



Edge Detection

- Gradient steepest along edges \rightarrow edge detection



Gradient Correction

$$\psi' = 10^{\log(\psi) - (a \times \log(\nabla g) - \bar{\nabla} g)}$$

$$\log(\psi) = a \times \log(\nabla g) + b$$

